Supporting Information

A multifunctional Zr-MOF for rapid removal of $Cr_2O_7^{2-}$, efficient gas adsorption/separation, and catalytic performance

Xiurong Zhang,[a] Xia Wang,[a] Weidong Fan,*[a] Yutong Wang,[a] Xiaokang Wang,[a] Kai Zhang,[a] and Daofeng Sun*[,a,b]

[a] College of Science, China University of Petroleum (East China), Qingdao, Shandong 266580, People's Republic of China.

[b] School of Materials Science and Engineering, China University of Petroleum (East China), Qingdao, Shandong 266580, People's Republic of China.

*Email: weidongfan@163.com; dfsun@upc.edu.cn

The supporting information contains 26 pages including 22 figures, 8 tables, and 1 scheme.

Table of Contents

1. Synthesis of H_4TB ligand.

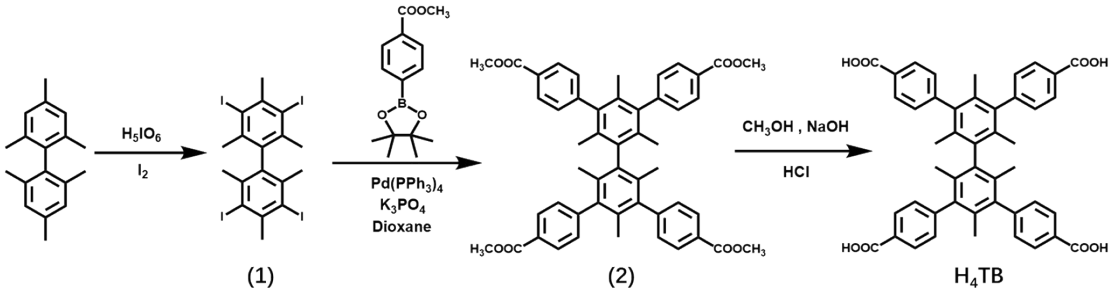

Scheme S1. Synthetic procedures of the H_4TB ligand.

1.1 Synthesis of 3,3',5,5'-tetraiodobimensityl (1)

To a mixture of AcOH (150 ml) and conc.H_2SO_4 (6 ml) was added bimesityl (2.0 g, 8.39 mmol), I_2 (s) (4.26 g, 16.77 mmol) and H_5IO_6 (1.91 g, 8.39 mmol). The mixture was heated at 70℃ for 3 h then cooled and poured over ice to form a pink precipitate. The precipitate was filtered and collected while the filtrate was extracted with $CHCl_3$, washed with 5% sodium thiosulfate, dried over $MgSO_4$, and concentrated under reduced, then recrystallized from ethyl acetate and pet ether mixture to obtain product as a colorless solid (4.37 g, Yield: 70%). ^{1}H NMR (400 MHz, $CDCl_3$): δ 2.09 (s, 12 H), 3.06 (s, 6 H). Anal. Calcd. For $C_{18}H_{18}I_4$ (MW 741): C, 29.14; H, 2.45. Found: C, 29.05; H, 2.39.

1.2 Synthesis of 3,3',5,5'-tetra((4-methoxycarbonyl)phenyl)bimesityl (2)

Tetraiodobimesityl (1.03 g, 1.38 mmol), methyl 4-(4,4',5,5'-tetramethyl-1,3,2-dioxaborolan-2-yl) benzoate (2.13 g, 6.62 mmol), $Pd(PPh_3)_4$ (0.48 g, 0.416 mmol) and K_3PO_4 (3.53 g, 16.6 mmol) were placed in a 250 ml two-necked round bottom flask under a N_2 gas atmosphere. The flask was further charged with a 200 ml of dry 1,4-dioxane, and the contents were heated for 48 h. After the mixture was cooled to room temperature, the solvent was removed, water was added. The water phase was washed with $CHCl_3$. The mixed organic phases were dried with $MgSO_4$. After the solvent was removed, the crude product was purified by column chromatography with $CHCl_3$ as the eluent (Yield: 62%). ^{1}H NMR (400 MHz, $CDCl_3$): δ 1.65 (s, 12H), 1.66 (s, 6H), 3.94 (s, 12H), 7.26 (d, 8H), 8.09 (d, 8H). Anal. Calcd. For $C_{50}H_{46}O_8$ (MW 774): C, 77.50; H, 5.98. Found: C, 77.38; H, 5.82.

1.3 Synthesis of 3,3',5,5'-tetra((4-carboxyphenyl)bimesityl (H_4TB)

2 (1.00 g, 1.29 mmol) was dissolved in 30 ml MeOH, 30 ml 2 mol/L NaOH aqueous solution was added. The mixture was stirred at 60℃ overnight. The organic phase was removed, the aqueous phase was acidified with diluted hydrochloric acid (2 mol/L, 20 ml) to give white precipitate, which was filtered and washed with water several times (Yield: 93%). ^{1}H NMR (400 MHz, DMSO-d6): δ 1.63 (s, 12H), 3.33 (s, 6H), 7.34 (d, 8H), 8.01 (d, 8H), 12.96 (s, 4H). Anal. Calcd. For $C_{46}H_{38}O_8$ (MW 719): C, 76.77; H, 5.28. Found: C, 76.62; H, 5.21.

2. Synthesis, Crystal data, structure and characterization of UPC-50.

Table S1. Crystal data and structure refinement of **UPC-50** with CCDC 1954445.

Identification code	**UPC-50**
Empirical formula	$C_{46}H_{46}O_{16}Zr_3$
Formula weight	1128.49
Temperature/K	150.01(10)
Crystal system	tetragonal
Space group	P4/mnc
a/Å	19.1184(5)
b/Å	19.1184(5)
c/Å	32.7397(13)
α/°	90
β/°	90
γ/°	90
Volume/Å^3	11966.8(8)
Z	4
ρ_{calc}g/cm^3	0.626
μ/mm^{-1}	2.337
F(000)	2280.0
2Θ range for data collection/°	8.482 to 133.128
Reflections collected	21932
Independent reflections	5380 [R_{int} = 0.1571, R_{sigma} = 0.1194]
Data/restraints/parameters	5380/0/156
Goodness-of-fit on F^2	0.987
Final R indexes [I>=2σ (I)]	R_1 = 0.0878, wR_2 = 0.2211
Final R indexes [all data]	R_1 = 0.1321, wR_2 = 0.2685
Largest diff. peak/hole / e Å^{-3}	1.66/-1.35

Table S2. Selected bond lengths (Å) and selected bond angles (º) for **UPC-50**.

Atom	Atom	Length/Å	Atom	Atom	Atom	Angle/°
Zr1	Zr2[1]	3.5027(14)	Zr2	Zr1	Zr2[1]	60.58(3)
Zr1	Zr2	3.5027(14)	Zr2	Zr1	Zr2[2]	91.01(5)
Zr1	Zr2[2]	3.5027(14)	Zr2[1]	Zr1	Zr2[2]	60.58(3)
Zr1	Zr2[3]	3.5027(14)	Zr2[2]	Zr1	Zr2[3]	60.58(3)
Zr1	O2[4]	2.174(7)	Zr2	Zr1	Zr2[3]	60.58(3)
Zr1	O2[1]	2.174(7)	Zr2[1]	Zr1	Zr2[3]	91.01(5)
Zr1	O2	2.174(7)	O1	Zr2	Zr1	117.3(2)
Zr1	O2[5]	2.174(7)	O1	Zr2	Zr1[2]	117.3(2)
Zr1	O6	2.153(9)	O1	Zr2	Zr2[3]	85.0(4)
Zr1	O6[5]	2.153(9)	O2	Zr1	Zr2[1]	109.75(19)
Zr1	O6[1]	2.153(9)	O2[4]	Zr1	Zr2[1]	74.87(19)
Zr1	O6[4]	2.153(9)	O2[3]	Zr1	Zr2[3]	74.87(19)
Zr2	Zr1[3]	3.5026(14)	O2[3]	Zr1	Zr2[2]	111.75(18)
Zr2	Zr2[1]	3.5336(18)	O2[5]	Zr1	Zr2[2]	74.87(19)
Zr2	Zr2[2]	3.5335(18)	O2[3]	Zr1	Zr2	109.75(19)
Zr2	O1	2.142(13)	O2[5]	Zr1	Zr2[1]	111.75(18)
Zr2	O3	2.205(14)	O2[5]	Zr1	Zr2	165.8(2)
Zr2	O6[6]	2.123(8)	O2	Zr1	Zr2[3]	111.75(18)
Zr2	O6[7]	2.136(8)	O2	Zr1	Zr2[2]	165.8(2)
Zr2	O6[1]	2.136(8)	O2[5]	Zr1	Zr2[3]	109.75(19)
Zr2	O6	2.123(8)	O2[4]	Zr1	Zr2	111.75(18)
Zr2	O4[6]	2.232(7)	O2[4]	Zr1	Zr2[3]	165.8(2)

Symmetry transformations used to generate equivalent atoms:

[1]+Y,1-X,-Z; [2]1-X,1-Y,-Z; [3]1-Y,+X,+Z; [4]+Y,1-X,+Z; [5]1-X,1-Y,+Z; [6]+X,+Y,-Z; [7]1-Y,+X,-Z; [8]1/2+Y,-1/2+X,1/2-Z; [9]1-X,-Y,+Z

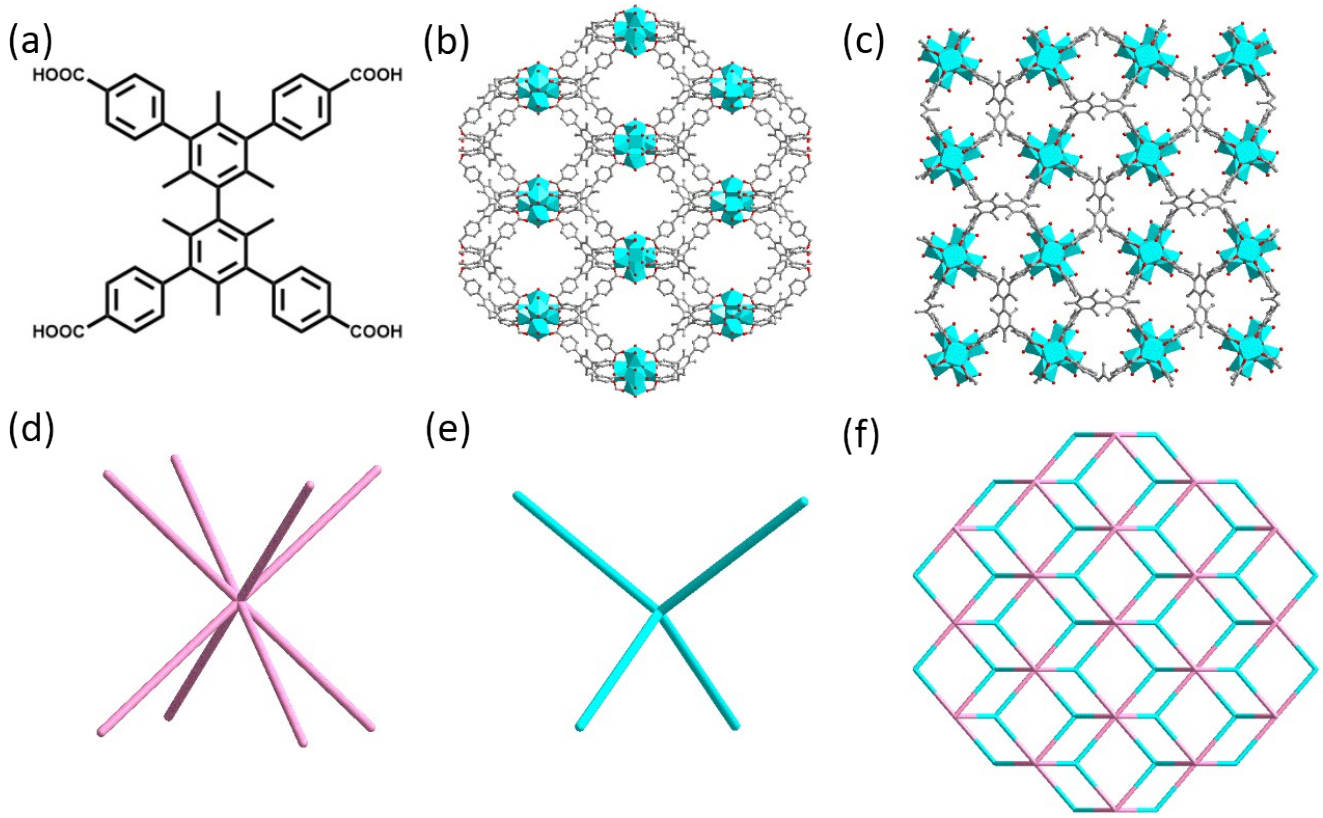

Figure S1. The structure of **UPC-50**: (a) Chemical structure of H_4TB ligand. (b) Three-dimensional open framework along the a-axis and b-axis. (c) Three-dimensional open framework along the c-axis. (d-f) The topological feature of **UPC-50**.

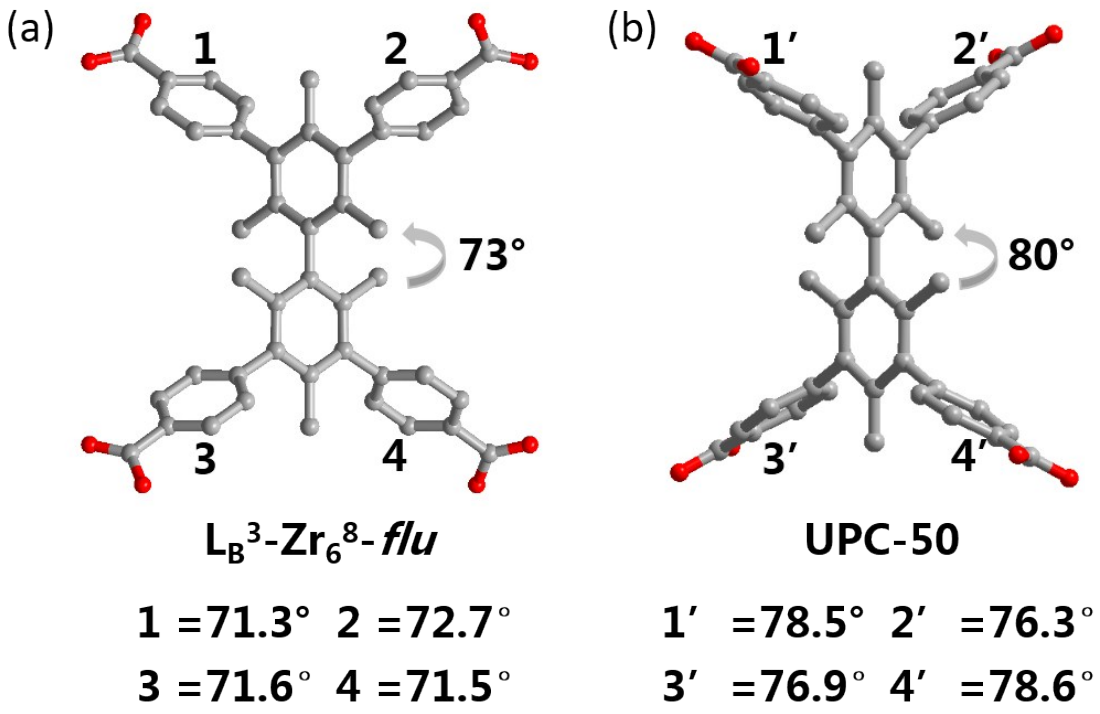

Figure S2. Torsion angle between benzene rings on ligands in **L_B^3-Zr_6^8-*flu*** (a) and **UPC-50** (b).

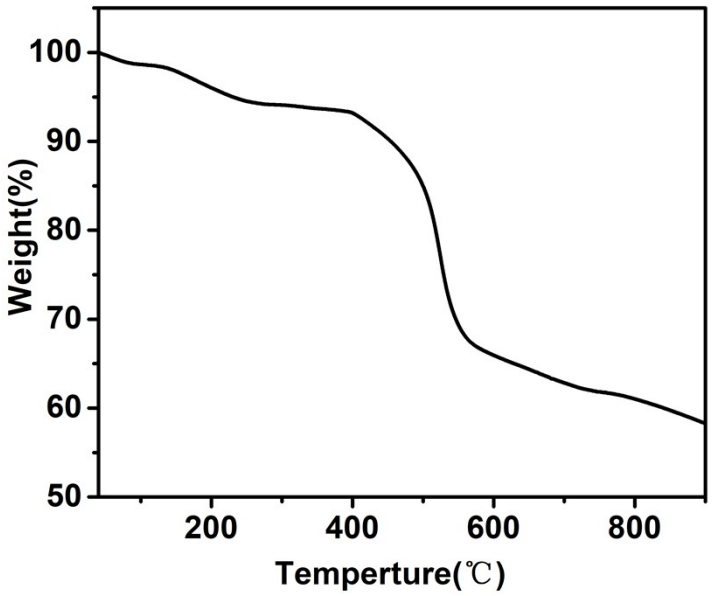

Figure S3. The TGA of **UPC-50**.

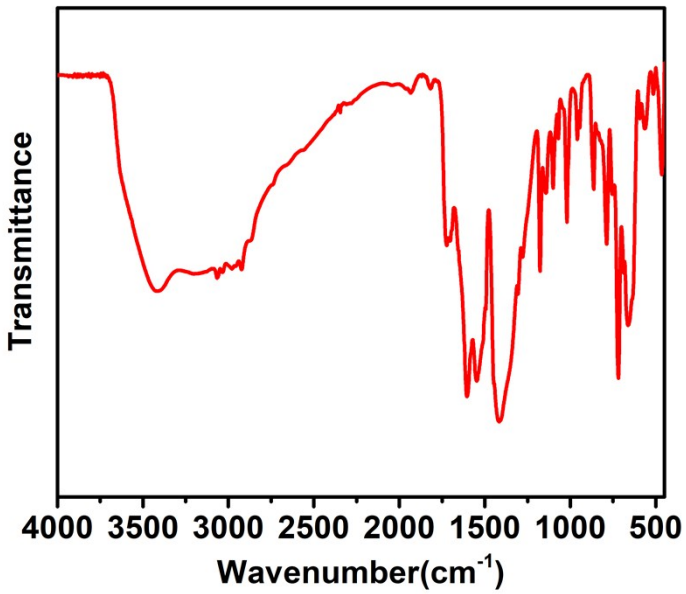

Figure S4. The IR of **UPC-50**.

3. $Cr_2O_7^{2-}$ adsorption of UPC-50.

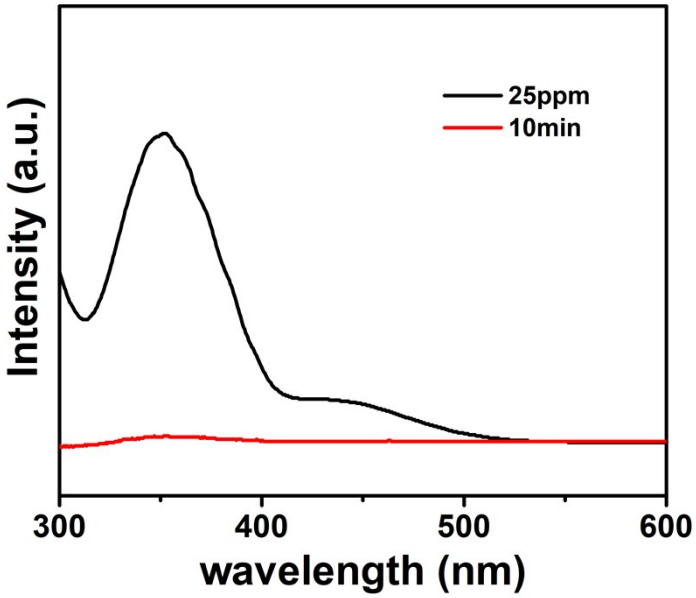

Figure S5. UV-vis spectra for the $Cr_2O_7^{2-}$ adsorption behavior at low concentration.

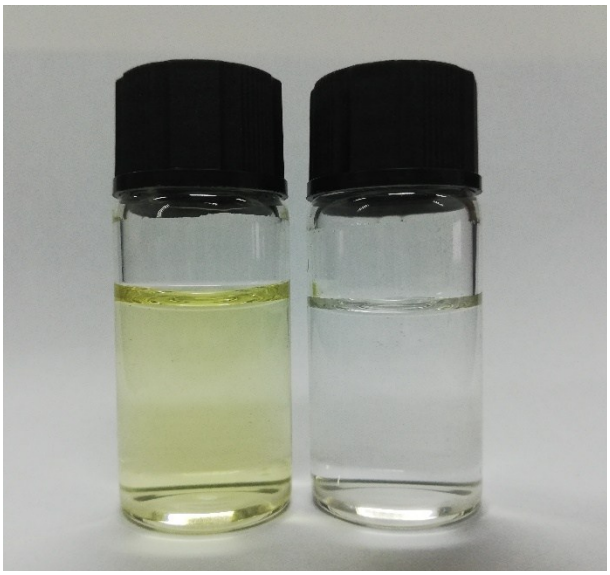

Figure S6. Photographs of the 25 ppm $Cr_2O_7^{2-}$ solution before and after adsorption.

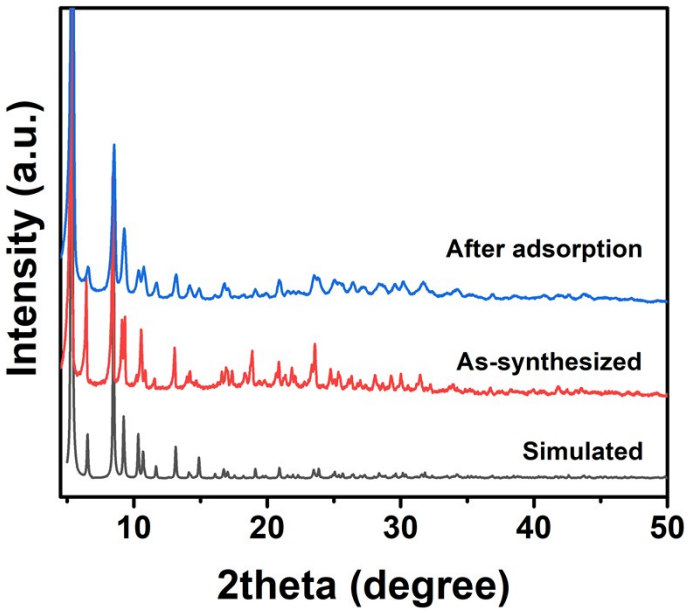

Figure S7. The PXRD of **UPC-50** before and after adsorption.

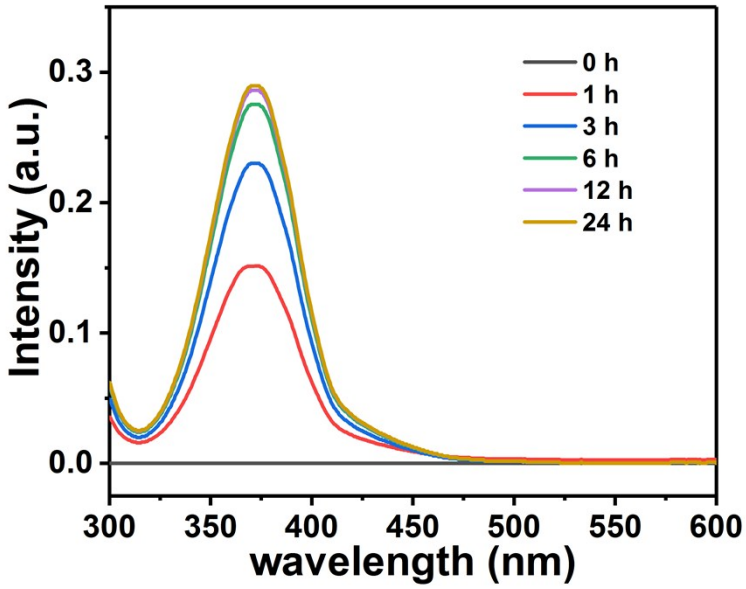

Figure S8. UV-vis spectra for the $Cr_2O_7^{2-}$ desorption behavior in aqueous solution at different time.

Table S3. Comparison of $Cr_2O_7^{2-}$ adsorption ability of **UPC-50** with other MOFs.

MOFs	q_{max} (mg/g)	time of equilibrium	removal rate (%)	Ion residue/initial concentration	Ref.
UPC-50	**56.8**	**<1 min**	**99.64**	**89ppb /25ppm**	**This work**
NU-1000	76.8	3 min	99.75	60ppb /50ppm	1
JLU-MOF60	149	90 min	99.92	20ppb /25ppm	2
TMU-30	145	10 min			3
ZIU-101	245	10 min			4
1-Cl	65.8	30 min			5
1-ClO_4	62.9	6 h			6
FIR-53	74.2	1 h			7
FIR-54	103	1 h			7
MOF-867	53.4	12 h			8
Ag-SLAG-21	60	48 h			9

4. Gas adsorption of UPC-50.

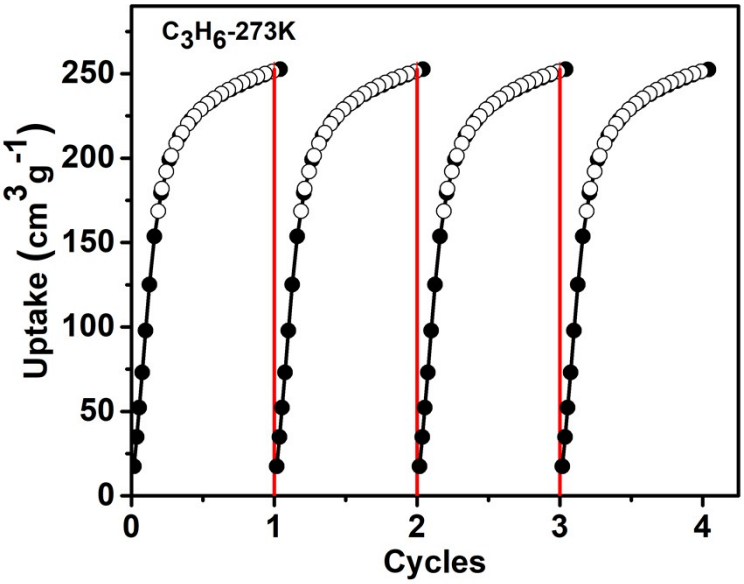

Figure S9. Cycles of C_3H_6 adsorption for **UPC-50** at 273 K.

Table S4. Single component gas adsorption Data for **UPC-50.**

Gas	T [K]	Amount [$cm^3\ g^{-1}$]	Amount [mmol g^{-1}]	Q_{st} [KJ mol^{-1}]
CH_4	273	15.21	0.68	8.23
	298	12.03	0.54	
C_2H_2	273	124.94	5.58	11.76
	298	73.42	3.28	
C_2H_4	273	103.71	4.63	13.43
	298	67.76	3.03	
C_2H_6	273	143.27	6.40	14.61
	298	90.50	4.04	
C_3H_6	273	252.67	11.28	18.72
	298	213.74	9.54	

Table S5. Adsorption selectivity of hydrocarbon at 1 bar for different molar fraction of binary mixtures.

Binary gas mixtures	Molar fraction	Selectivity (273 K)	Selectivity (298 K)
C_3H_6/CH_4	50:50	78.28	40.03
	10:90	54.10	29.39
C_3H_6/C_2H_2	50:50	5.87	5.24
	10:90	7.02	5.10
C_3H_6/C_2H_4	50:50	6.66	5.96
	10:90	7.62	5.69
C_3H_6/C_2H_6	50:50	4.43	4.13
	10:90	5.14	4.27
C_2H_2/CH_4	50:50	8.42	7.45
	10:90	8.82	7.87
C_2H_4/CH_4	50:50	7.79	6.48
	10:90	7.81	6.63
C_2H_6/CH_4	50:50	11.16	8.50
	10:90	10.00	8.33

Table S6. Comparison of Separation ratio of C_3H_6/CH_4 for Selected MOFs.

MOFs	Molar fraction	Selectivity (273 K)	Selectivity (298 K)	Ref.
UPC-50	**10:90**	**50.10**	**23.39**	**This work**
	50:50	**78.28**	**40.03**	
UPC-33	10:90	87.69	24.76	10
	50:50	228.34	42.4	
UPC-32	10:90	22.56	33.93	11
	50:50	19.83	31.46	
UPC-99	50:50	496.7	306.9	12
MFM-202a	50:50	74 (293 K)		13
UTSA-35a	50:50	90 (296 K)		14

Table S7. Comparison of Light Hydrocarbon Adsorption Data for Selected MOFs.

MOFs	T	CH_4	C_2H_2	C_2H_4	C_2H_6	C_3H_6	ref
UPC-50	**273**	**15.21**	**124.94**	**103.71**	**143.27**	**252.67**	**This work**
	298	**12.03**	**73.42**	**67.76**	**90.50**	**213.74**	
UPC-102	273	21.2	85.7	68.9	89.8	148.8	15
	298	9.4	70.6	56.4	74.0	142.0	
UPC-33	273	9.7	65.1	43.6	51.8	114.2	10
	298	7.0	44.3	31.1	35.0	94.3	
FJI-C1	273		135.9	85.2	123.6		16
	298	9.7	93.8	64.0	87.4		
FJI-C4	273	32.7	82.8	70.1	73.4		17
	298	18.4	72.5	61.4	66.3		
1-mim	273	14.65	119.42	92.37	101.03		18
	298	10.64	76.26	64.95	79.91		
1-eim	273	19.32	117.84	87.30	99.35		18
	298	11.48	73.70	61.29	75.38		
1-pim	273	16.24	101.42	84.54	93.78		18
	298	9.70	65.00	53.72	71.65		
1-buim	273	14.08	93.54	73.16	81.77		18
	298	8.86	56.14	48.70	63.00		
UPC-99	273	18.9	75.1	87.4	92.7	127.5	12
	298	9.8	43.1	44.3	61.0	119.5	
UPC-21	273	43.2	196.5	123.1	137.6	124.1	19
	298	25.7	139.5	98.4	104.3	110.1	
UPC-35	273	11.0	72.5	56.4	70.1	138.1	20
	298	4.8	44.4	35.9	40.9	118.3	
M'MOF-20	273		95.0	53.0			21
	298	8.0	81.0	44.0	49.0		

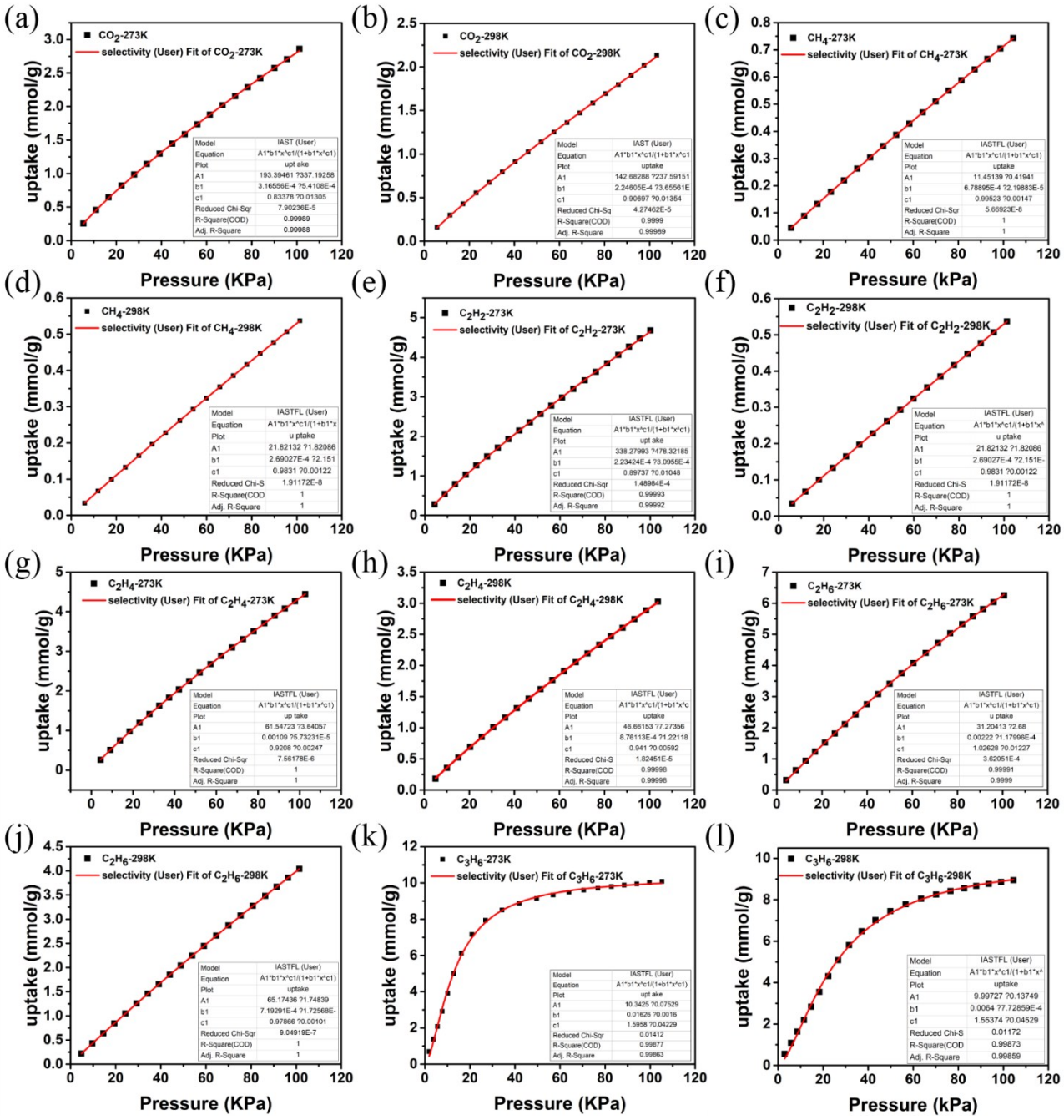

Figure S10. The parameters and optimized adsorption isotherms of CO_2 (a and b), CH_4 (c and d), C_2H_2 (e and f), C_2H_4 (g and h), C_2H_6 (i and j), and C_3H_6 (k and l) for calculated selectivity by using IAST method at 273 K and 298 K, respectively.

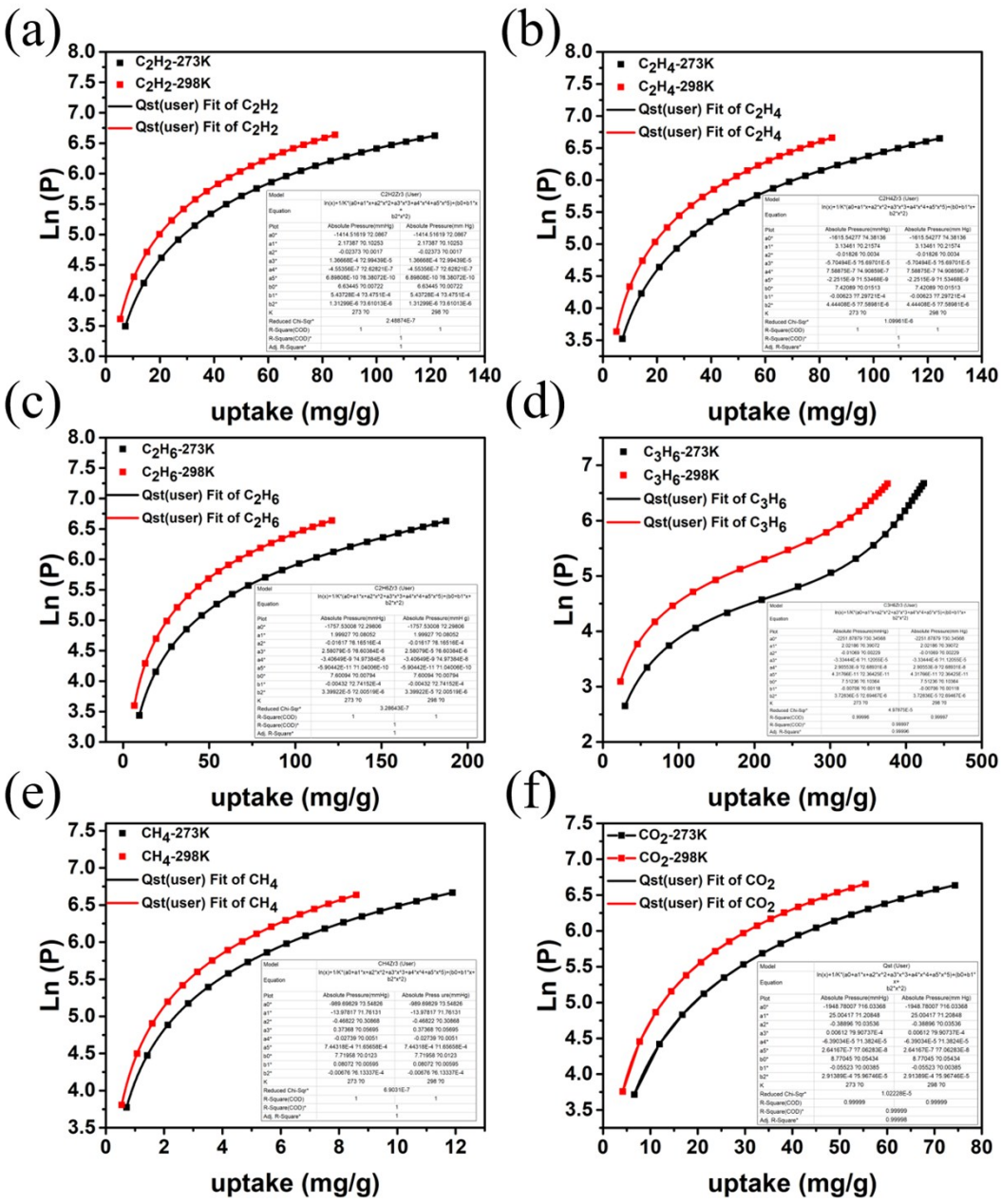

Figure S11. The parameters and optimized adsorption isotherms for calculated Q_{st} of C_2H_2 (a), C_2H_4 (b), C_2H_6 (c), C_3H_6 (d), CH_4 (e), and CO_2 (f) using a variant of the Clausius-Clapeyron equation.

5. Catalytic Cycloaddition of CO_2 with Epoxides of UPC-50.

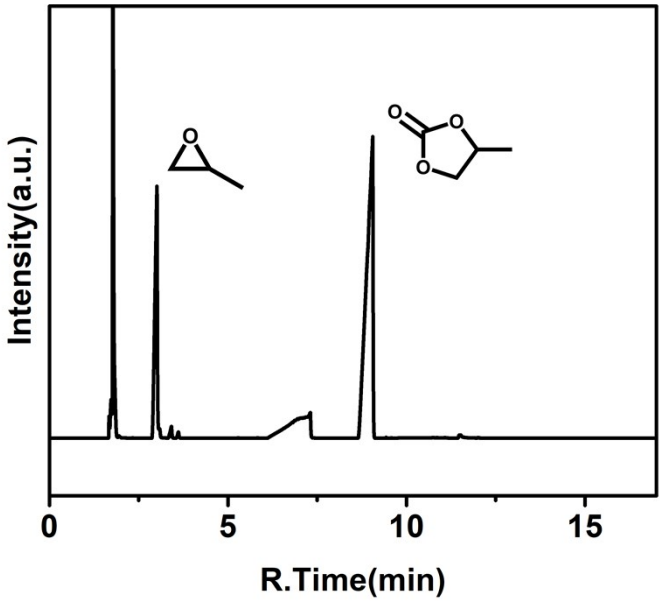

Figure S12. The GC spectrum for heterogeneous nature of catalysis in reaction of Propylene carbonate at room temperature and 1 bar. **MS** $[M+H]^+$: 102.0317.

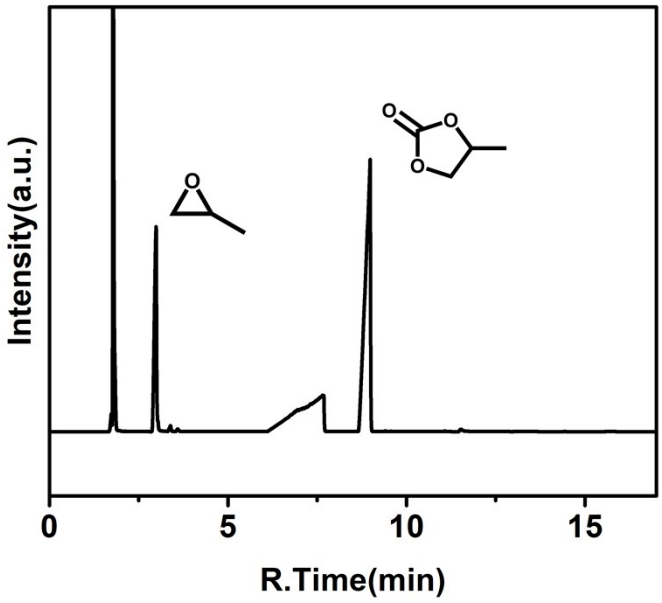

Figure S13. The GC spectrum for heterogeneous nature of catalysis in reaction of Propylene carbonate at 50°C and 6 bar. **MS** $[M+H]^+$: 102.0317.

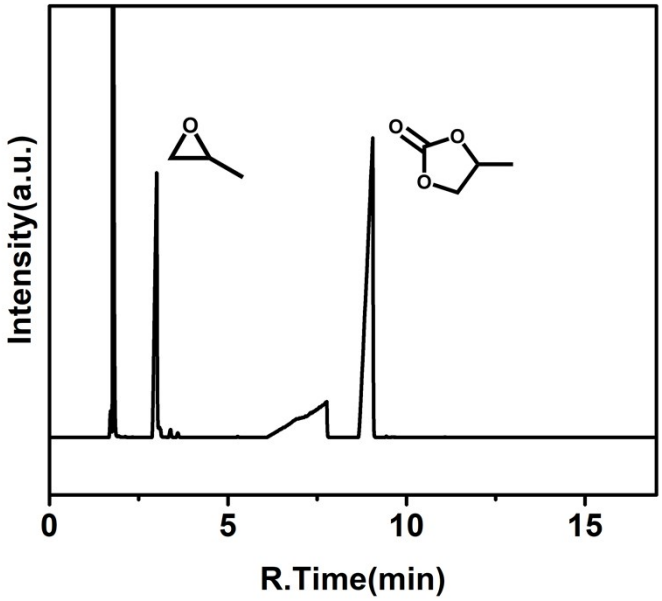

Figure S14. The GC spectrum for heterogeneous nature of catalysis in reaction of Propylene carbonate at 50°C and 6 bar after one recycle. **MS** $[M+H]^+$: 102.017.

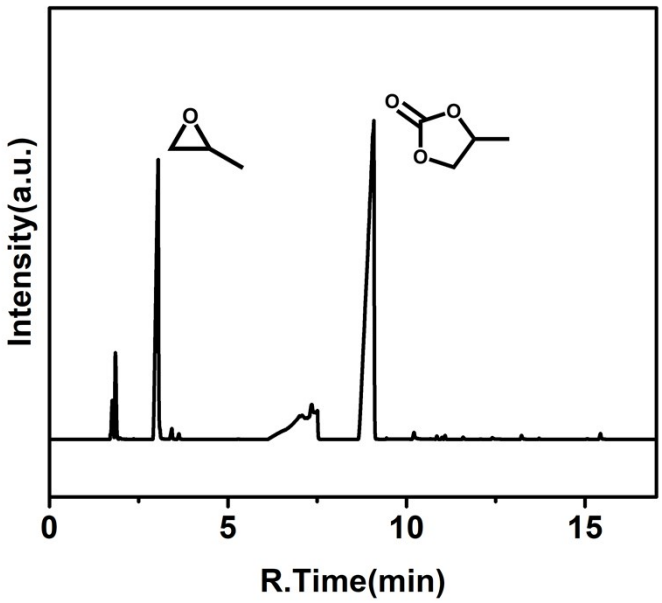

Figure S15. The GC spectrum for heterogeneous nature of catalysis in reaction of Propylene carbonate at 50°C and 6 bar after two recycle. **MS** $[M+H]^+$: 102.017.

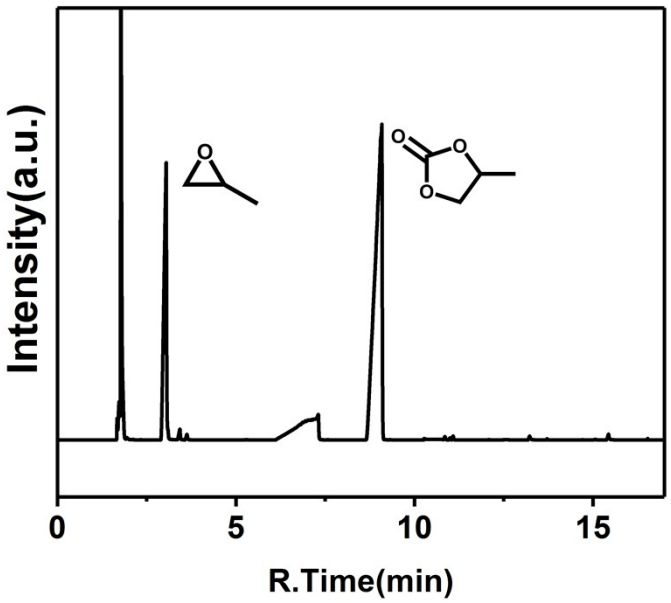

Figure S16. The GC spectrum for heterogeneous nature of catalysis in reaction of Propylene carbonate at 50°C and 6 bar after three recycle. **MS** $[M+H]^+$: 102.017.

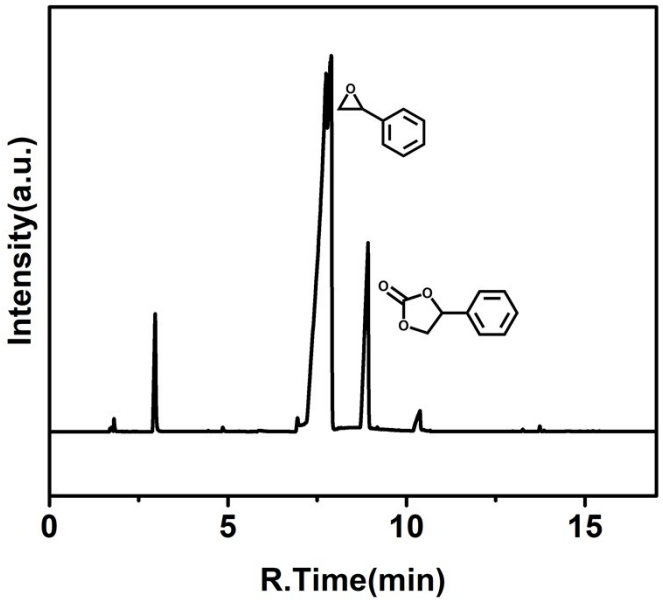

Figure S17. The GC spectrum for heterogeneous nature of catalysis in reaction of 4-phenyl-1,3-dioxolan-2-one at 50°C and 6 bar. **MS** $[M+H]^+$: 164.0473.

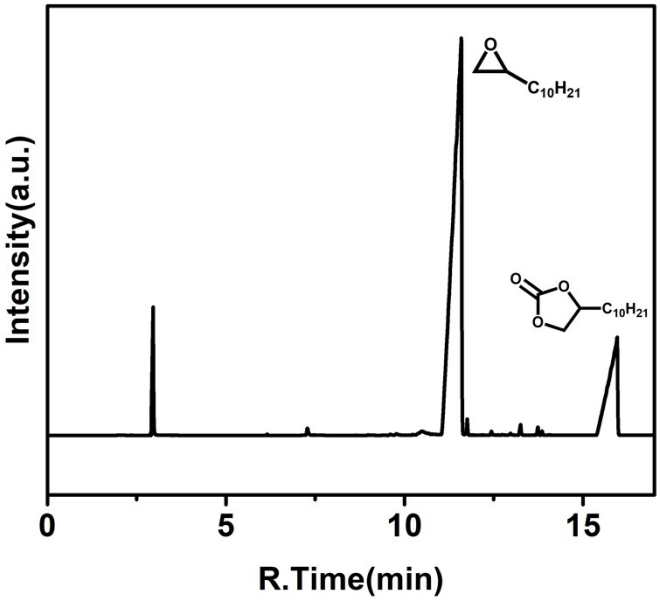

Figure S18. The GC spectrum for heterogeneous nature of catalysis in reaction of 4-decyl -1,3-dioxolan-2-one at 50°C and 6 bar. **MS** $[M+H]^+$: 228.1725.

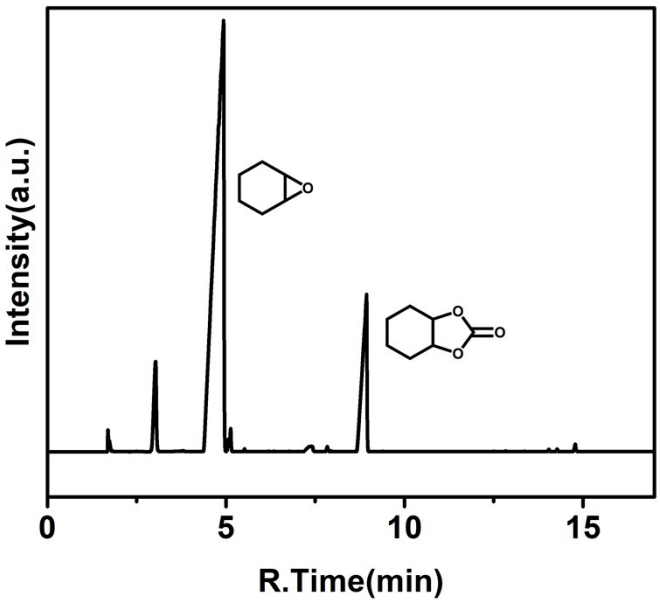

Figure S19. The GC spectrum for heterogeneous nature of catalysis in reaction of hexahydrobenzo[d][1,3]dioxol-2-one at 50°C and 6 bar after two recycle. **MS** $[M+H]^+$: 142.0630.

Table S8. Comparison of catalysts performances in the cycloaddition of CO_2 with different epoxides for selected MOFs.

MOF	Catalytic type	T (℃)	P (bar)	Time (h)	Yields (%)	ref
UPC-50	**1(R=CH_3)**	**25**	**1**	**24**	**65.97**	**This work**
	1(R=CH_3)	**50**	**6**	**5**	**75.08**	**This work**
	2(R=Ph)	**50**	**6**	**5**	**32.16**	**This work**
	3(R=$C_{10}H_{21}$)	**50**	**6**	**5**	**20.34**	**This work**
ZIF-8	2	100	7	5	54	22
Co-MOF	1	25	1	48	57.1	23
MOF-505	1	25	1	48	48.0	24
HKUST-1	1	25	1	48	49.2	24
ZIF-95	1	80	12	2	76	25
MOF-53	1	100	16	2	78	26
NH_2-MIL-125	1	100	20	6	85	27
ZnMOF-1-NH_2	1	80	8	8	89	28
UiO-66	1	50	10	12	77	29
UiO-66-NH_2	1	50	10	12	42	29
HL-7	1	25	1	48	75.5	30
MMPF-9	1	25	1	48	87.4	31

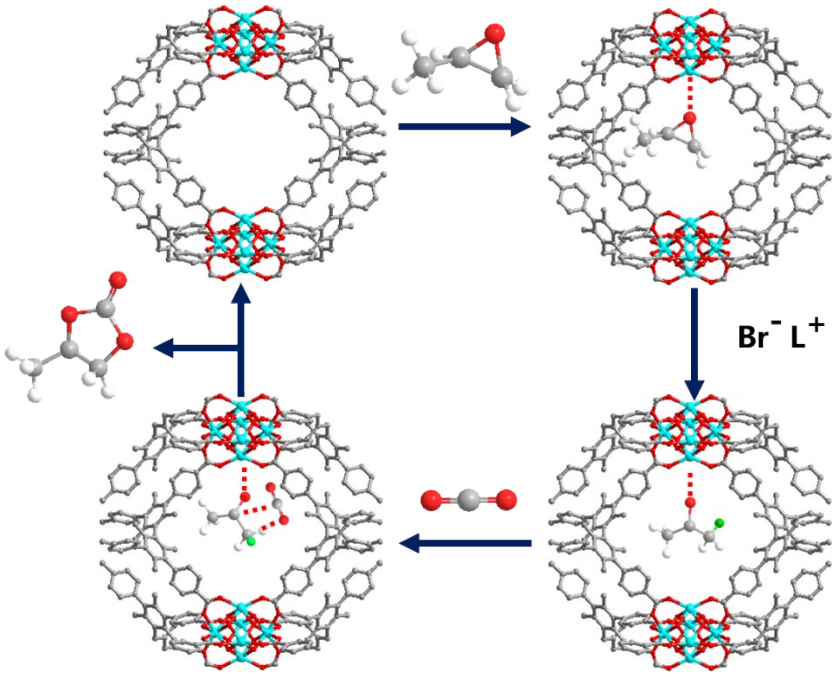

Figure S20. The catalytic mechanism for the cycloaddition of CO_2 with epoxides into cyclic carbonates catalyzed by **UPC-50** (The green ball represents the Br^-; L^+ =tetra-n-tertbutylammonium).

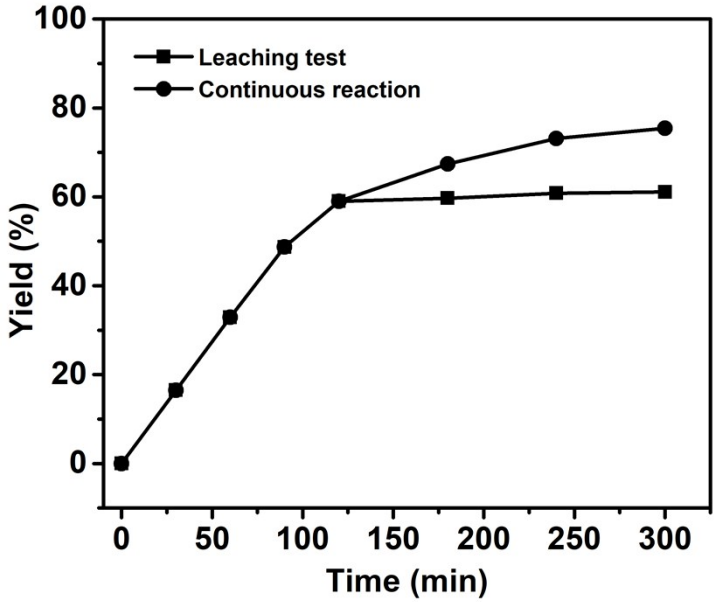

Figure S21. Evidence of heterogeneous nature of catalysis in carbon dioxide cycloaddition reactions. (●) Continuous reaction; (■) catalyst was removed after 120 minutes.

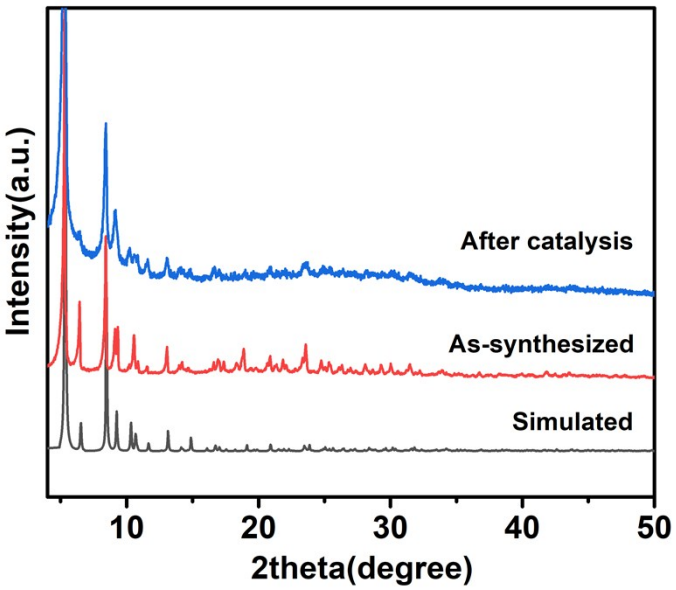

Figure S22. The PXRD of **UPC-50** before and after catalysis.

References

1. Z.J. Lin, H.Q. Zheng, H.Y. Zheng, L.P. Lin, Q. Xin and R. Cao. Inorg. Chem. 2017, 56, 14178-14188.
2. J.M. Liu, Y. Ye, X.D. Sun, B. Liu, G.H. Li, Z.Q. Liang and Y.L. Liu. J. Mater. Chem. A. 2019, 7, 16833-16841.
3. L. Aboutorabi, A. Morsali, E. Tahmasebi and O. Büyükgüngor. Inorg. Chem. 2016, 55, 5507-5513.
4. Q. Zhang, J.C. Yu, J.F. Cai, L. Zhang, Y.J. Cui, Y. Yang, B.L. Chen and G.D. Qian. Chem. Commun. 2015, 51, 14732–14734.
5. L. Ma, J. Yang, B.B. Lu, C.P. Li and J.F. Ma. Inorg. Chem. 2018, 57, 11746-11752.
6. P. Shi, B. Zhao, G. Xiong, Y. Hou and P. Cheng. Chem. Commun. 2012, 48, 8231-8233.
7. H.R. Fu, Z.X. Xu and J. Zhang. Chem. Mater. 2015, 27, 205-210.
8. Q. Zhang, J. Yu, J. Cai, L. Zhang, Y. Cui, Y. Yang, B. Chen and G. Qian. Chem. Commun. 2015, 51, 14732-14734.
9. H. Fei, C.S. Han, J.C. Robins and S.R.J. Oliver. Chem. Mater. 2013, 25, 647-652.
10. W.D. Fan, Y.T. Wang, Q. Zhang, A. Kirchon, Z.Y. Xiao, L.L. Zhang, F.N. Dai, R.M. Wang, and D.F. Sun. Chem. Eur. J. 2017, 23, 1-8.
11. W.D. Fan, Y.T. Wang, Z.Y. Xiao, Z.D. Huang, F.N. Dai, R.M. Wang and D.F. Sun. Chinese Chem. Lett. 2018, 29, 865-868.
12. X. Wang, X.R. Zhang, K. Zhang, X.K. Wang, Y.T. Wang, W.D. Fan and F.N. Dai. Inorg. Chem. Front. 2019, 6, 1152-1157.
13. S. Gao, C.G. Morris, Z.Z. Lu, Y. Yan, H.G.W. Godfrey, C. Murray, C.C. Tang, K.M. Thomas, S.H. Yang and M. Schröder. Chem. Mater. 2016, 28, 2331-2340.
14. Y. He, Z. Zhang, S. Xiang, F.R. Fronczek, R. Krishna, B. Chen. Chem. Commun. 2012, 48, 6493-6495.
15. W.D. Fan, X. Wang, B. Xu, Y.T. Wang, D.D. Liu, M. Zhang, Y.Z. Shang, F.N. Dai, L.L. Zhang, and D.F. Sun. J. Mater. Chem. A. 2018, 6, 24486-24495.
16. Y.B. Huang, Z.J. Lin, H.R. Fu, F. Wang, M. Shen, X.S. Wang, and R. Cao. ChemSusChem. 2014, 7, 2647-2653.

17. L. Li, X.S. Wang, J. Liang, Y.B. Huang, H.F. Li, Z.J. Lin, and R. Cao. ACS Appl. Mater. Interfaces. 2016, 8, 9777-9781.

18. H.R. Fu and J. Zhang. Inorg. Chem. 2016, 55, 3928-3932.

19. M.H. Zhang, X.L. Xin, Z.Y. Xiao, R.M. Wang, L.L. Zhang and D.F. Sun. J. Mater. Chem. A. 2017, 5, 1168-1175.

20. Y.T. Wang, W.D. Fan, X. Wang, Y.F. Han, L.L. Zhang, D. Liu, F.N. Dai, and D.F. Sun. Inorg, Chem. Front. 2018, 5, 2408-2412.

21. N. Sikdar, S. Bonakala, R. Haldar, S. Balasubramanian, and T.K. Maji. Chem. Eur. J. 2016, 22, 6059-6070.

22. M.Q. Zhu, D. Srinivas, S. Bhogeswararao, P. Ratnasamy and M.A. Carreon. Catal. Commun. 2013, 32, 36-4.

23. H.H. Wang, L. Hou, Y.Z. Li, C.Y. Jiang, Y.Y. Wang and Z.H. Zhu. ACS Appl. Mater. Interfaces. 2017, 9, 17969-17976.

24. W.Y. Gao, Y. Chen, Y.H. Niu, K. Williams, L. Cash, P.J. Perez, L. Wojtas, J.F. Cai, Y.S. Chen and S.Q. Ma. Angew. Chem. Int. Ed. 2014, 53, 2615-2619.

25. E.E. Macias, P. Ratnasamy and M.A. Carreon. Catal. Today. 2012, 198, 215-218.

26. J. Kim, S.N. Kim, H.G. Jang, G. Seo and W.S. Ahn. Appl. Catal. A Gen. 2013, 453, 175-180.

27. J. Melendez, M. North, P. Villuendas and C. Young. Dalton Trans. 2011, 40, 3885-3902.

28. R.R. Kuruppathparambil, R. Babu, H.M. Jeong, G.Y. Hwang, G.S. Jeong, M.I. Kim, D.W. Kim and D.W. Park. Green Chem. 2016, 18, 6349-6356.

29. J. Noh, Y. Kim, H. Park, J. Lee, M. Yoon, M.H. Park, Y. Kim and M. Kim. J. Ind. Eng. Chem. 2018, 64, 478-483.

30. X.L. Zhang, H.L. Liu, D.S. Zhang and L.L. Gen. Inorg. Chem. Commun. 2019, 101, 184-187.

31. W.Y. Guo, Y. Chen, Y. Niu, K. Williams, L. Cash, P.J. Perez, L. Wojtas, J. Cai, Y.S. Chen and S. Ma. Angew. Chem. Int. Ed. 2014, 53, 2615-2619.